ACS OMEGA

http://pubs.acs.org/journal/acsodf

Article

Application of Machine Learning in a Mineral Leaching Process—Taking Pyrolusite Leaching as an Example

Zheng Zhang, Xianming Zhang, Dan Zhang, Xingran Zhang,* Facheng Qiu, Wensheng Li, Zuohua Liu, Jiancheng Shu, and Chengli Tang

Cite This: *ACS Omega* 2022, 7, 48130−48138

Read Online

ACCESS | Metrics & More | Article Recommendations | Supporting Information

ABSTRACT: In this study, several machine learning models were used to analyze the process variables of electric-field-enhanced pyrolusite leaching and predict the leaching rate of manganese, and the applicability of those models in the leaching process of hydrometallurgy was compared. It showed that there was no correlation between the six leaching conditions; in addition to the leaching time, the concentrations of sulfuric acid and ferrous sulfate had great influences on the leaching of pyrolusite. The results of the prediction models showed that the support vector regression model has the best prediction performance, with regression index (R^2) = 0.92 and mean square error = 25.04, followed by the gradient boosting regression model (R^2 > 0.85). In this research, machine learning models were applied to the optimization of the manganese leaching process, and the research process and methods were also applicable to other hydrometallurgical processes for majorization and result prediction.

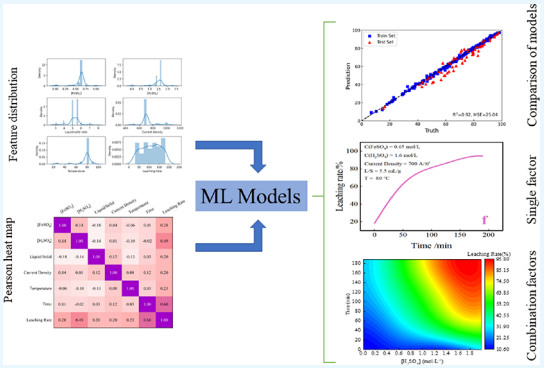

1. INTRODUCTION

Manganese (Mn) and manganese compounds, as important industrial materials, play a signification role in various industrial fields, but due to the large demand for extensive use, the storage of high-grade manganese ore resources has declined,[1,2] while the low-grade pyrolusite still retains huge storage capacity.[3] In order to meet the demand of industrial production, it is necessary to efficiently utilize low-grade pyrolusites.

In order to improve the leaching rate of pyrolusite and utilize various materials efficiently, many efficient leaching methods were proposed, such as electric-field-enhanced leaching, microwave leaching, biological leaching, etc. By studying the leaching mechanism of pyrolusite with an electric field,[4,5] it has been found that both the consumption of ferrous sulfate and the acid leaching reagent sulfuric acid could be reduced under electric field enhancement. Luo et al.[6] combined ball milling and an electric field to make the optimal leaching rate of pyrolusite reach 97.79%. Chen et al.[7] used pyrite as a reducing agent to leaching pyrolusite under microwave conditions, and the leaching rate reached 93.03%. Lan et al.[8] applied bioleaching pyrolusite, which proved that the leaching rate can be as high as 98%.

In recent years, with the advancement of computing power, big data, and algorithms, artificial intelligence technology has been used in various areas, such as molecular and material chemistry prediction,[9−11] the discovery and synthesis of new materials,[12,13] and environmental pollution removal prediction.[14] In the field of hydrometallurgy, machine learning techniques have also been applied industrially. Hoseinian et al.[15] used an artificial neural network combined with a genetic algorithm to predict the leaching rate of copper oxide ore pillars and investigated the effect of various conditions in the leaching process on the copper recovery rate. The coefficient of determination of the model and the predicted mean square error were 0.96 and 0.02, respectively, and the model was combined with the leaching process to optimize the leaching effect. Xie et al.[16] used a radial basis function neural network with a self-adjusting structure to effectively predict the iron ion concentration at the output of the hydrometallurgical zinc industry, and the root-mean-square error of the model prediction was 0.215 g/L, which compensated for the information delay caused by the inability to detect the iron ion concentration online in real time. In addition, random forests, decision trees, SVM, and extreme gradient boosting were also used in metallurgy and metal recycling.[17−21]

Machine learning for mineral extraction prediction in the metallurgical industry is little studied for different machine learning models with the analysis of leaching process conditions for minerals such as manganese. In this paper, the correlation

Received: September 22, 2022
Accepted: December 6, 2022
Published: December 14, 2022

https://doi.org/10.1021/acsomega.2c06129
ACS Omega 2022, 7, 48130−48138

between each leaching condition and the importance of leaching conditions on the leaching rate were investigated by the Pearson correlation coefficient and multiple linear regression models, which were used to guide leaching optimization and condition selection. Several machine learning models driven by electrically enhanced pyrolusite leaching data predicted the leaching rate and analyzed the applicability of different machine learning models. The effects and trends of single leaching conditions and combined leaching conditions on leaching rates were analyzed visually to improve the understanding of the leaching process by the prediction models.

2. DATA PROCESSING AND MACHINE LEARNING MODELS

2.1. Data Processing. *2.1.1. Dataset.* The experimental data of electric-field-enhanced pyrolusite leaching were from the published papers in 2015[4] and 2017,[5] with 304 sets of data samples. The liquid−solid ratio (mL/g), current density (A/m^2), leaching temperature (°C), and leaching time (min) are the same conditions in both datasets, while the remaining conditions in the 2015 dataset, which are the mass ratio of ferrous sulfate heptahydrate to pyrolusite and the mass ratio of sulfuric acid to pyrolusite, were different from those of the 2017 dataset, so they should be converted into ferrous sulfate concentration and sulfuric acid concentration by the liquid−solid ratio to keep consistent with the 2017 dataset.

The conversion equations are

$$c(\mathrm{FeSO_4}) = \frac{(m_{\mathrm{FeSO_4\cdot 7H_2O}}: m_{\mathrm{MDO}}) \times 1000}{n_{\mathrm{FeSO_4\cdot 7H_2O}} \times (l/g)} \tag{1}$$

$$c(\mathrm{H_2SO_4}) = \frac{(m_{\mathrm{H_2SO_4}}: m_{\mathrm{MDO}}) \times 1000}{n_{\mathrm{H_2SO_4}} \times (l/g)} \tag{2}$$

The test and training sets of the data were randomly divided into a ratio of 8:2, and the optimal model selection was determined using 10-fold cross-validation on the overall dataset. The distribution of each feature and the results of 10-fold cross-validation are plotted in the Supporting Information.

2.1.2. Standardization of Dataset Features. The data were centered and scaled to standardize by the mean (u) and standard deviation (s) of each condition to eliminate the influence of the unit magnitude between the leaching conditions on the machine model and improve the machine learning models.

Data normalization equation:

$$\mathrm{New\_}x_i = \frac{(x_i - u)}{s} \tag{3}$$

where x_i represents the sample of different leaching conditions and i is the sequence number of the observation, such as 1, 2, 3, ..., n.

2.2. Machine Learning Models. *2.2.1. Multiple Linear Regression Models.* Multiple linear regression[21−23] is a statistical tool for fitting linear relationships between independent and dependent variables and can be used to identify linear relationships between single or multiple variables. Simple linear regression consists of a single element input, and multiple linear regression consists of multiple inputs.

$$X_b = \begin{Bmatrix} 1 & b_1^{(1)} & \cdots & b_n^{(1)} \\ 1 & b_1^{(2)} & \ddots & b_n^{(2)} \\ \vdots & \vdots & \vdots & \vdots \\ 1 & b_1^{(m)} & \cdots & b_n^{(m)} \end{Bmatrix} \tag{4}$$

$$\theta = (\theta_1 + \theta_2 + \cdots + \theta_i)^T = (X_b^T \times X_b^{-1})^{-1} X_b^T y \tag{5}$$

where X_b is the feature matrix, $b_n^{(m)}$ is the feature m of the nth data sample in the data sample, θ is the coefficient vector, and y is the actual value. The prediction results can be calculated by the following equation.

$$y_{\mathrm{pred}} = x_i \times \theta \tag{6}$$

Namely,

$$y = \theta_0 + \theta_1 x_1 + \theta x_2 + \cdots + \theta_n x_n \tag{7}$$

y represents the output of the model, x_i (i = 1,2, ...n) represents the input features, and θ is the coefficient term of the input features of the equation. The optimization objective of multiple linear regression is to obtain the optimal coefficient θ vector set corresponding to the minimum value of the sum of distances of the equation to all input data. In this study, a multiple linear regression model containing a constant term was developed for the importance analysis of leaching conditions based on the electric-field-enhanced leaching data.

2.2.2. Support Vector Machine Regression Model. A support vector machine (SVM)[24,25] is a supervised machine learning model that can handle classification and regression problems. The processing method of the SVM is to use nonlinear kernel functions to map input features into a high-dimensional space to linear separability to solve linear inseparability problems in a low-dimensional space. The application of the SVM in regression is called support vector regression (SVR).

SVR trained by train = $\{(\vec{x}_1, \hat{y}_1), (\vec{x}_2, \hat{y}_2), \ldots(\vec{x}_i, \hat{y}_i)\}(i = 1,2, \ldots, N)$ compares the difference between the model's output $f(\vec{x}_i) = y_i$ and the true value $\hat{y}_i$ with the given parameter ε. If $|f(\vec{x}_i) = y_i| \geq \varepsilon$, the loss calculation will be performed; otherwise, the prediction is correct.

$$\min_{\vec{w}, b} \frac{1}{2} \|\vec{w}\|_2^2 + C\sum_{i=1}^{N} L_\varepsilon(f(\vec{x}_i) - \hat{y}_i) \tag{8}$$

where C is the penalty term hyperparameter given before the model is built ($C \geq 0$) and L_ε is the loss function.

The optimization of SVR can be performed by introducing relaxation variables ξ_i and $\hat{\xi}_i$ with the "soft boundary" to control and constrain the model, and the optimized expression is

$$\min_{\vec{w}, b, \xi_i, \hat{\xi}_i} \frac{1}{2} \|\vec{w}\|_2^2 + C\sum_{i=1}^{N} (f(\vec{x}_i) - \hat{y}_i) \tag{9}$$

$$\text{s. t. } f(\vec{x}_i) - \hat{y}_i \leq \varepsilon + \xi_i \tag{10}$$

$$\hat{y}_i - f(\vec{x}_i) \leq \varepsilon + \hat{\xi}_i \tag{11}$$

$$\xi_i \geq 0, \hat{\xi}_i \geq 0, i = 1, 2, \ldots, N \tag{12}$$

SVR is a nonlinear machine learning model, where it is easier to fit the nonlinear relationship between features and predicted values in the small samples than other machine learning models,

https://doi.org/10.1021/acsomega.2c06129
ACS Omega 2022, 7, 48130−48138

and has a strong generalization ability and can solve high-dimensional data problems. In this study, the penalty term C = 100 and the radial basis function (rbf) is determined by grid search to train the data for prediction.

2.2.3. Decision Tree Model. A decision tree (DT)[26,27] is a supervised learning machine that makes decisions based on some logical rules, which does not depend on the predefined relationship between input features and predicted output results, ignoring the magnitude of input features. The decision tree is divided by searching features to pursue the effect of uniform output distribution, and the output of the decision tree is optimized by parameters. For example, grid search and Bayesian optimization[28] of the minimum leaf size are used to obtain good prediction results, and dropping nodes are used to prevent overfitting of the decision tree.

Decision tree division criteria are based on the information gain, gain rate, Gini index, etc. The division criterion has a great impact on the size of leaf nodes and the depth of layers of decision trees, but it has a limited impact on its generalization ability.[29] In this study, the parameters were determined by grid search, and the quality of division was measured by mean absolute error (MAE); the best splitting strategy was selected using best, the depth of the tree was set to 20, and the minimum number of samples of leaf nodes was set to 2.

2.2.4. Random Forest Model. A random forest[30] (RF) is a machine learning model, an ensemble of decision trees, which handles classification and regression problems efficiently. In contrast to the traditional decision tree, which selects the optimal attributes from the current set of nodes as a division standard, the random forest selects k attribute nodes randomly from the current set of nodes and divides the optimal attributes from the remaining subsets, in which the randomness is determined by the parameter k. The random selection of the subset of attributes without selecting from all attributes results in a higher training efficiency.

When a random forest initially has only one base learner, it is a decision tree model with random selection generating perturbations, which is characterized by poor performance, poor fitting, low generalization ability, etc. Multiple stochastic decision tree models are integrated in parallel by Bagging,[31] and the results are predicted by voting or averaging between each base learning model. In this study, random forest parameters were determined by grid search, the number of base models was 100, the quality of attribute partitioning was measured using mean square error (MSE), and the default values were used for the remaining parameters.

2.2.5. Multilayer Perceptron Model. A multilayer perceptron (MLP)[32−35] or deep feedforward network is a typical deep artificial neural network (ANN), inspired by the human neuronal system for processing information. The MLP is approximated with a mapping function between input features and output predictions.

The MLP contains a simple neuron interconnection system, which is divided into at least three layers, which are input and output layers, with one or more hidden layers in the middle. The neurons in the input layer do not participate in the calculation, just passing the input data to the hidden layer, and the neurons in the other layers complete the nonlinear transformation by activation functions (e.g., logistic, tanh, and relu) to complete the resultant output of that layer.

The two consecutive layers of neurons are connected by the weight θ obtained during the training process, which approximates the mapping function between input and output. The MLP is supervised learning, and $f(\vec{x}_i, \theta)$ is approximated to the actual value $\hat{y}_i$ by training the approximation function f, where the difference between $f(\vec{x}_i, \theta)$ and $\hat{y}_i$ is the error value, which is used for the training process to adjust the weights θ, thereby reducing the overall network error.

The MPL network has the possibility of global non-convergence, and the model is particularly sensitive to the given parameters. The activation function, the number of hidden layers, the number of neurons in each layer, the number of iterations, and the overfitting prevention regularization between the layers all have a great influence on the model. In order to obtain a high prediction regression effect, this study uses grid search to adjust the parameters and then determines logistics as the activation function, with 4 hidden layers, the number of neurons in each hidden layer is 80, and the learning rate is set to adaptive to construct the prediction model.

2.2.6. Gradient Boosting Regression Model. The gradient boosting regressor (GBR)[36,37] is a model using the boosting forward algorithm to train a base learning model with an initial training set, and the subsequent model training combines the performance of the base learning model to adjust the distribution of training samples. During training, in order to achieve the effect of paying more attention to wrong samples in the basic learning model, the residual gradient of the previous model is reduced according to the minimized loss function and improves the prediction accuracy of the model step by step.

In this study, according to grid search, the number of decision regression trees was 200, the learning rate was 0.1, the maximum depth of each decision regression number was 5, and the minimum number of samples in each internal node of the tree was 4. The mean square error (MSE) was used to measure the quality of attribute classification, the minimum absolute deviation (lad) was used as the loss function, and the rest of the parameters were set as default parameters.

2.3. Correlation Coefficient and Evaluation Criteria.

2.3.1. Pearson's Correlation Coefficient. Pearson's correlation coefficient[38] expresses the linear relationship between variables, which contributes to observing the effect of leaching conditions on the predicted results and provides guidance on the optimization of the variables. Pearson's correlation coefficient was verified and compared with the leaching conditions calculated in the machine learning model and played a role of mutual corroboration.

$$P\_\text{value} = \frac{\sum_{i=1}^{n}(X_i - \overline{X})(Y_i - \overline{Y})}{\sqrt{\sum_{i=1}^{n}(X_i - \overline{X})^2}\sqrt{\sum_{i=1}^{n}(Y_i - \overline{Y})^2}} \tag{13}$$

where X_i and Y_i represent the sample with different leaching conditions and $\overline{X}$ and $\overline{Y}$ represent the mean of different leaching conditions.

2.3.2. Evaluation Criteria. In the study, the coefficient of determination (R^2) and mean square error (MSE) were selected as the evaluation criteria to find out the excellent prediction models among the machine learning models.

$$R^2 = 1 - \frac{\sum(y_i - \hat{y}_i)}{\sum(y_i - \mu_y)} \tag{14}$$

where y_i denotes the model output value, $\hat{y}_i$ denotes the actual value of the model, μ_y denotes that the y is the mean value of the model, and i is the ordinal number of the observation, such as 1, 2, 3, ..., n.

https://doi.org/10.1021/acsomega.2c06129
ACS Omega 2022, 7, 48130−48138

$$\mathrm{MSE} = \frac{1}{n}\sum_{i=1}^{n}(y_i - \hat{y}_i) \tag{15}$$

R^2 was used to represent the performance of the model to evaluate the degree of conformity between the predicted value of the model and the actual value. MSE was used to explain the magnitude of the error. The above two performance indicators can effectively evaluate the prediction effect of the model.

3. RESULTS AND DISCUSSION

3.1. Feature Correlation and Importance Analysis. As shown in the Pearson correlation coefficient heat map (Figure 1), the lighter color between the parts indicates the weak

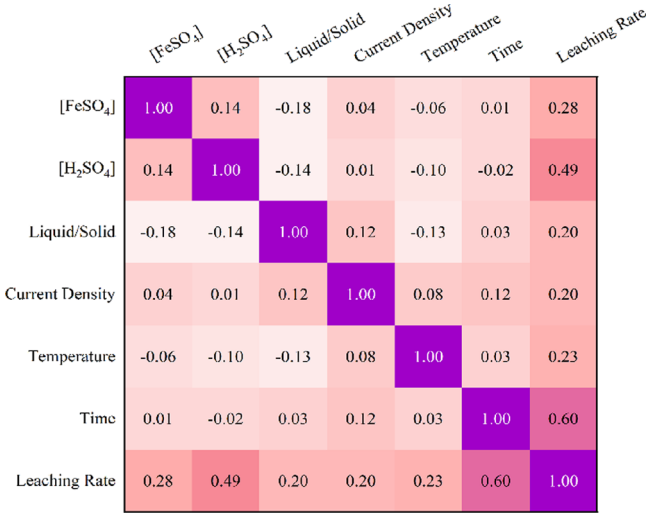

Figure 1. Pearson correlation coefficient heat map for leaching conditions.

correlation between the leaching conditions, and there is no cumulative contribution to the prediction of the leaching rate. The leaching conditions with darker colors in the leaching rate row of Figure 1 are the leaching time, sulfuric acid concentration, and ferrous sulfate concentration, indicating that the above conditions have a greater impact on the leaching rate.

The standardized leaching conditions were subjected to a multiple linear regression with the leaching rate data, and the fitted equation is

$$y = 0.277x_1 + 0.538x_2 + 0.336x_3 + 0.043x_4 + 0.32x_5 + 0.558x_6 + 3.9 \times 10^{-16} \tag{16}$$

where $x_1 - x_6$ represent the ferrous sulfate concentration, sulfuric acid concentration, liquid−solid ratio, current density, temperature, and leaching time, respectively.

The larger coefficients in front of the leaching conditions in the equation were leaching time and sulfuric acid concentration, which were close to the Pearson correlation coefficient heat map, and the importance of the above two leaching conditions was consistent with Zhang et al.[4]

The importance score analysis according to the GBR model for leaching conditions (Figure 2) revealed that the leaching time has the greatest influence on the leaching effect in the electric-field-enhanced pyrolusite leaching process, which was due to the fact that the pyrolusite acid leaching process is a liquid−solid reaction, which is a nucleation reduction model.[39] The acid leaching reaction occurred on the surface of pyrolusite,

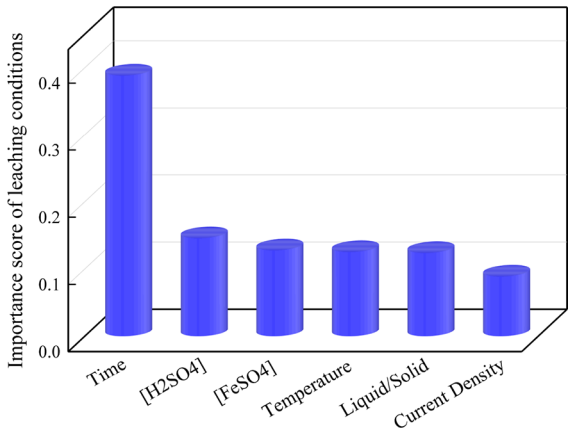

Figure 2. Importance score of leaching conditions.

while the reaction has not yet occurred inside the mineral. With the increase of reaction time, the leaching of the mineral inside gradually contacted with the liquid surface, and thus, the leaching rate gradually increased. The second most important factor was the sulfuric acid concentration. A higher acid concentration promoted the reduction of manganese dioxide by ferrous ions, thereby promoting the leaching of manganese. The third most important factor was the concentration of ferrous sulfate, in which Fe^{2+} has a strong reducing property, which can reduce high-valent manganese and thus improve the leaching.[5]

3.2. Comparison of the Model Prediction Ability. The leaching rate was predicted by a multiple linear regression model, a support vector regressor model, a decision tree model, a random forest model, a multilayer perceptron model, and a gradient boosting model after determining the parameters by grid search. The multiple linear regression model (Figure 3a) exhibited poor results ($R^2 < 0.8$) on the test set, indicating that leaching of pyrolusites was a complex nonlinear process, which is consistent with the study of Zhang et al.[4] The prediction effect of the decision tree model (Figure 3c) was also relatively poor ($R^2 < 0.8$) with overfitting, indicating that the division of the decision tree by reducing the information entropy or the Gini index could not predict the leaching rate accurately. The low correlation between each leaching condition and the leaching rate, accounting for individual leaching condition data, could not accurately determine the leaching rate.

The random forest model (Figure 3d) and the gradient boosting regression model (Figure 3f) belong to the ensemble model, which integrates multiple weak learning models for voting prediction, which obtains relatively good prediction results, with R^2 of 0.87 and 0.88, respectively. The multilayer perceptron model (Figure 3e) lacks stability in the prediction process because the grid search determines the parameter learning_rate = adaptive, thus contributing to the learning rate change during the training process and the prediction effect change, but several experiments showed that the multilayer perceptron model prediction effect R^2 mean value was 0.87.

The support vector regression model (Figure 3b) had the best prediction effect ($R^2 = 0.92$, MSE = 25.04), and it had a good fitting ability on both the training and test sets. It indicated that the support vector regression model had the best prediction effect on the electric-field-enhanced leaching of pyrolusite with a good generalization ability. The support vector regression model was used for the subsequent study on the effect of leaching conditions on the leaching rate.

https://doi.org/10.1021/acsomega.2c06129
ACS Omega 2022, 7, 48130−48138

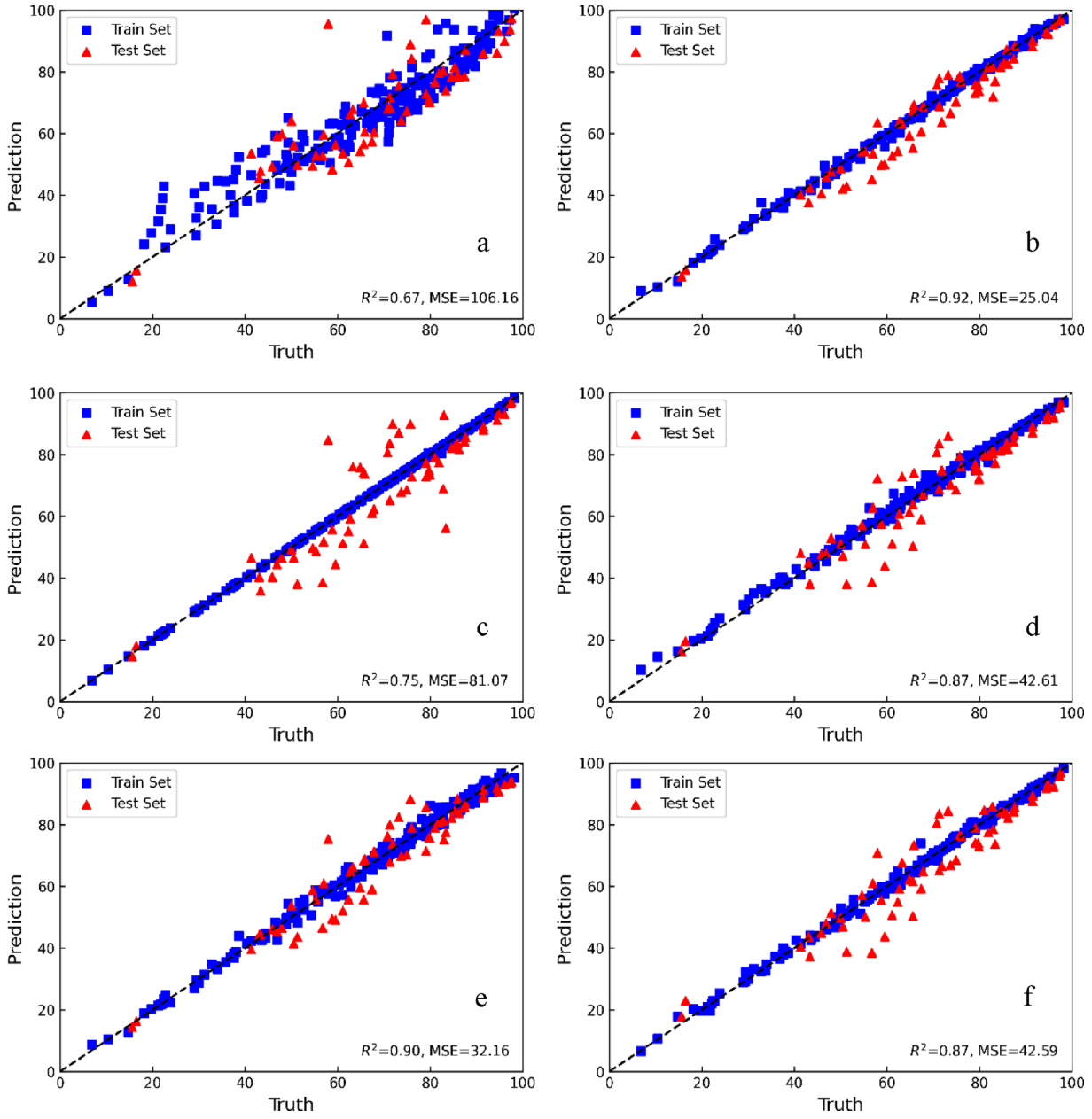

Figure 3. Comparisons between different models for prediction of the leaching rate and the evaluation criteria for the test set (train set:test set = 8:2): (a) multivariate linear model; (b) support vector machine; (c) decision tree; (d) random forest; (e) multilayer perceptron; (f) gradient boosting regression model.

3.3. Influence of Leaching Conditions on the Leaching Effect. *3.3.1. Effect of Single Leaching Conditions on the Leaching Rate.* The trend of the leaching rate under single factor conditions was examined by the method of controlled variables. The increase of ferrous sulfate concentration (Figure 4a) improves the leaching of manganese, which is due to the reducibility of Fe^{2+} ions, which can promote the reductive leaching of high-valent manganese. In addition, the leaching of manganese still occurs in the absence of ferrous ions, which is caused by the direct reduction of high-valent manganese by the electric field.[6] When the concentration of sulfuric acid is low (Figure 4b), the leaching rate of manganese remains low, which is due to the existence of colloidal alkaline ferric sulfate in the reaction solution under the environment of low-concentration sulfuric acid, which affects the leaching effect. When the sulfuric acid concentration increased, the colloidal basic iron sulfate is converted into iron sulfate, the solution mass transfer capacity increases, and the leaching effect is improved.[40] The increase of the liquid−solid ratio (Figure 4c) leads to an increase in the leaching rate of manganese, improving ion migration and the movement space of particles.[7] However, the improvement of the leaching effect is no longer obvious after the liquid−solid ratio reaches 5.5 mL/g. The increase of current density (Figure 4d) can significantly improve the leaching rate of manganese. After the current density increases from 500 to 950 A/m^2, the leaching rate increases to 98%, but it still does not reach 100% at around 1000 A/m^2, which is due to the MnO_2 attached to the anode after the oxidation of Mn^{2+}.[41] As the leaching temperature increases (Figure 4e), the leaching rate of manganese also increases. The molecules in the leaching reaction solution are heated and activated, involved in more reaction, and the surface reaction rate is proportional to the temperature.[42] The increase

https://doi.org/10.1021/acsomega.2c06129
ACS Omega 2022, 7, 48130−48138

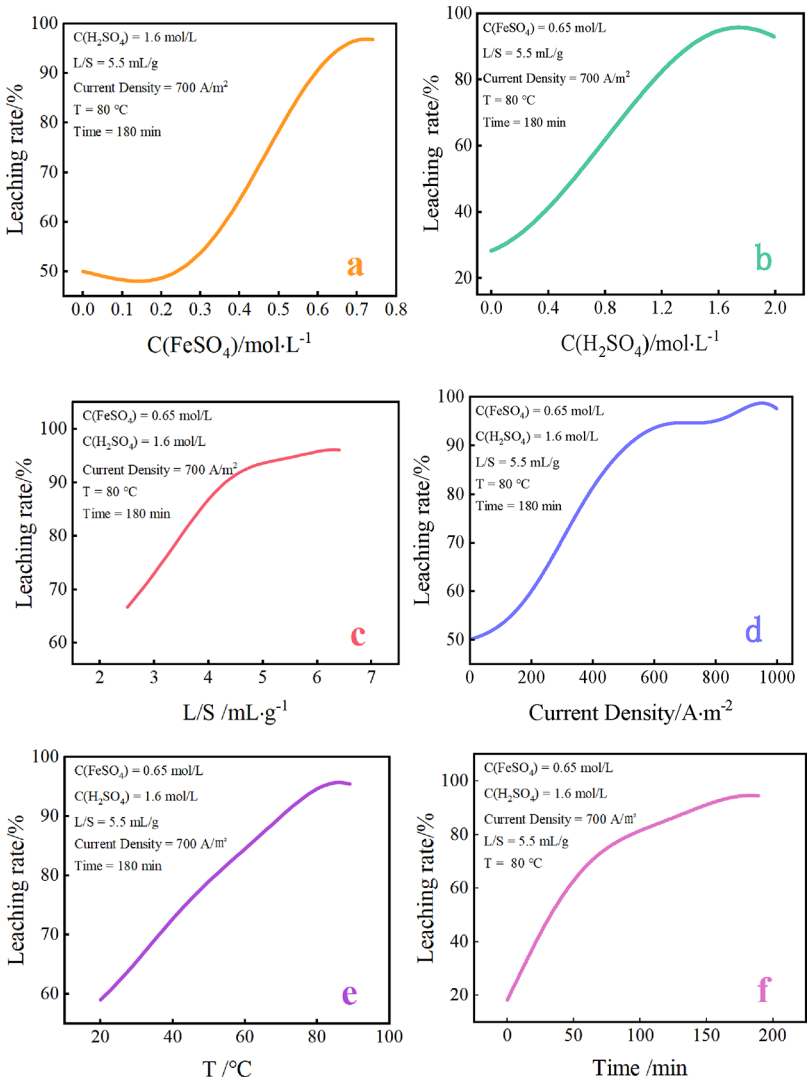

Figure 4. Influence of leaching conditions on the leaching rate. (a) Ferrous ion concentration; (b) sulfuric acid concentration; (c) liquid-to-solid ratio; (d) current density; (e) leaching temperature; (f) leaching time.

in the leaching rate with time is due to the gradual completion of the reaction (Figure 4f).

3.3.2. Effect of the Combination of Leaching Conditions on the Leaching Rate. According to Figure 5a, with the increase of the ferrous sulfate concentration and sulfuric acid concentration, the leaching rate of pyrolusite gradually increased generally. Comparing the effects of the concentration changes of the two reactants on the leaching rate of pyrolusite, it is found that when the concentrations of the ferrous sulfate concentration and sulfuric acid are lower than 0.5 and 0.8 mol/L, respectively, the change of other leaching conditions has no effect on the change of the leaching effect and the leaching rate is lower than 70%, indicating that neither sulfuric acid nor ferrous sulfate at low concentrations can leach manganese sufficiently. The low leaching rate at a low concentration of sulfuric acid is due to the formation of colloidal basic ferric sulfate,[40] which hinders the mass transfer. The low leaching rate at a low concentration of ferrous sulfate is due to the insufficient reducing agent involved in the reaction.

It can be seen from Figure 5b that with the increase of the concentration of ferrous sulfate, the leaching effect shows an upward trend first and then tends to be gentle. When the concentration of ferrous sulfate is lower than 0.5 mol/L, it is difficult to improve the leaching effect by increasing the liquid-to-solid ratio, which is caused by the insufficient reducing agent in the reaction system.[5] When the concentration of ferrous sulfate is higher than 0.5 mol/L, the effect of the liquid−solid ratio on the leaching effect is gradually clear. In addition, the change of the ferrous sulfate concentration at a high liquid−solid ratio has more obvious effects on the leaching rate, which is caused by improving the mass transfer effect and increasing the space for particle movement at a high liquid−solid ratio.[7]

The leaching rate observed by Figure 5c increased continuously with the increase of leaching time, but the increasing trend gradually flattened after the time reached 160 min. As shown in Figure 5c, when the sulfuric acid concentration is lower than 1 mol/L, the leaching rate always remains at low levels and there is no response to the increase in leaching time.

Figure 5d shows that a higher liquid−solid ratio and current density can obtain a higher leaching rate, but the increase of the leaching rate does not improve the leaching rate obviously after the current density reaches 900 A/m^2, while the energy consumption continues to increase. When the liquid−solid ratio is lower than 3.5 mL/g, the increase of current density cannot improve the leaching rate significantly and the leaching

https://doi.org/10.1021/acsomega.2c06129
ACS Omega 2022, 7, 48130−48138

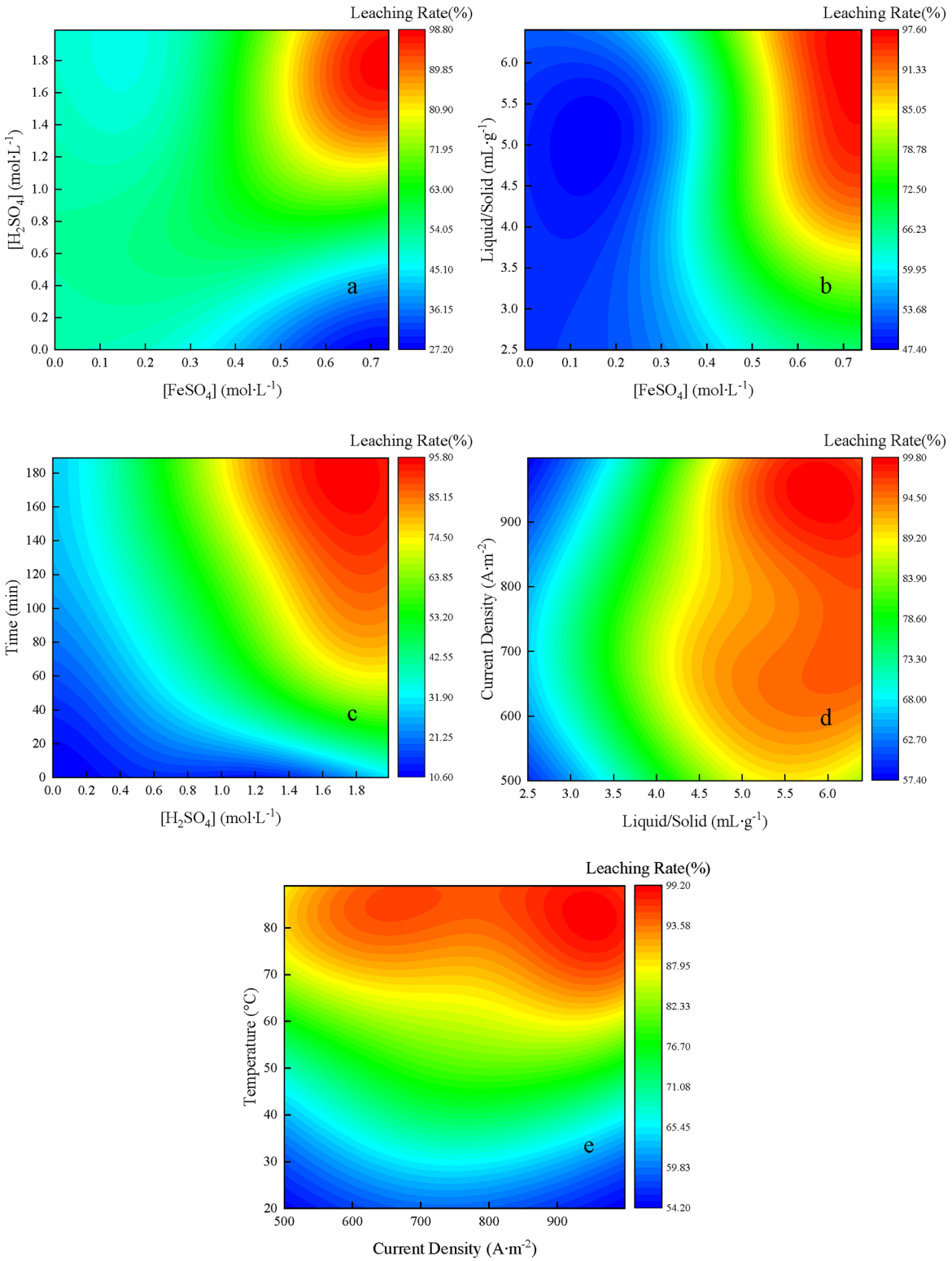

Figure 5. Effect of combination of leaching conditions on the leaching rate. (a) Influence of the concentration of ferrous sulfate and concentration of sulfuric acid. (b) Influence of the liquid-to-solid ratio and the concentration of ferrous sulfate on the leaching rate. (c) Influence of the leaching time and the concentration of sulfuric acid on the leaching rate. (d) Influence of the current density and the liquid-to-solid ratio on the leaching rate. (e) Influence of temperature and current density on the leaching rate.

rates is lower than 75%, which is caused by the viscous reaction system with a low liquid−solid ratio and poor mass transfer.[5]

Figure 5e illustrates that when the temperature is higher than 70 °C and the current density is higher than 500 A/m^2, the leaching rate will be higher than 90%, showing that an appropriate current density at a higher temperature can achieve good leaching results. Meanwhile, the leaching reaction does not require a particularly high reaction temperature with the action of an electric field, and a considerable leaching rate can be obtained because the electric field reduces the apparent

https://doi.org/10.1021/acsomega.2c06129
ACS Omega 2022, 7, 48130−48138

activation energy of the pyrolusite leaching process.[41] In addition, excessive current density will increase the energy consumption, but it will not significantly increase the leaching rate or even reduce the performance. This is owing to the fact that leached manganese ions are oxidized to MnO_2 and adsorbed on the anode, resulting in a decrease in the leaching rate.[4]

4. CONCLUSIONS

Through the comparison of machine learning models driven by pyrolusite leaching data, it revealed that the linear model predicted poorly indicating the complex nonlinearity of electric-field-enhanced pyrolusite leaching. The remaining machine learning models had better prediction results, of which the support vector regression model had the best prediction ability (R^2 = 0.92, MSE = 25.04), indicating the feasibility of machine learning models to predict leaching products in the field of hydrometallurgy. In addition, by studying various leaching conditions, it was found that the more important conditions are the leaching time, sulfuric acid concentration, and ferrous sulfate concentration. The leaching effect can be changed effectively by adjusting the above conditions. This study combined the field of hydrometallurgy with machine learning and used data visualization to analyze the influence and change trend of each leaching condition on the leaching rate. This study has important guiding significance for the intelligent research of hydrometallurgy.

■ ASSOCIATED CONTENT

Supporting Information

The Supporting Information is available free of charge at https://pubs.acs.org/doi/10.1021/acsomega.2c06129.

Distribution of each feature; results of 10-fold cross validation and the dataset used in this paper (Figure S1 and Tables S1−S3) (PDF)

■ AUTHOR INFORMATION

Corresponding Author

Xingran Zhang − *School of Chemistry and Chemical Engineering, Chongqing University of Technology, Chongqing 400054, China; Engineering Research Center for Waste Oil Recovery Technology and Equipment, Ministry of Education, Chongqing Technology and Business University, Chongqing 400067, China; School of Chemistry and Chemical Engineering, Chongqing University, Chongqing 400044, China;* orcid.org/0000-0001-6186-9613; Phone: +86 13140322555; Email: zhangxingran@cqut.edu.cn

Authors

Zheng Zhang − *School of Chemistry and Chemical Engineering, Chongqing University of Technology, Chongqing 400054, China*

Xianming Zhang − *Engineering Research Center for Waste Oil Recovery Technology and Equipment, Ministry of Education, Chongqing Technology and Business University, Chongqing 400067, China*

Dan Zhang − *School of Chemistry and Chemical Engineering, Chongqing University of Technology, Chongqing 400054, China*

Facheng Qiu − *School of Chemistry and Chemical Engineering, Chongqing University of Technology, Chongqing 400054, China*

Wensheng Li − *School of Chemistry and Chemical Engineering, Chongqing University of Technology, Chongqing 400054, China*

Zuohua Liu − *School of Chemistry and Chemical Engineering, Chongqing University, Chongqing 400044, China;* orcid.org/0000-0003-4229-0168

Jiancheng Shu − *Key Laboratory of Solid Waste Treatment and Resource Recycle (SWUST), Ministry of Education, Southwest University of Science and Technology, Mianyang 621010, China*

Chengli Tang − *Chongqing Chemical Industry Vocational College, Chongqing 401228, China*

Complete contact information is available at: https://pubs.acs.org/10.1021/acsomega.2c06129

Notes

The authors declare no competing financial interest.

■ ACKNOWLEDGMENTS

The authors gratefully acknowledge financial support from the "Science and Technology Research Program of Chongqing Municipal Education Commission" (no. KJQN202101132), the "Postgraduate Innovation Project of Chongqing University of Technology" (clgycx 20202054 and gzlcx 20223141), the "Scientific Research Project of Chongqing University of Technology" (no. 2017ZD46), the "National Natural Science Foundation of China" (no. 51804062), the "Youth Project of Science and Technology Research Program of Chongqing Education Commission of China" (no. KJQN202004504), and the "Chongqing Education Commission Science and Technology-funded major projects" (KJZD-M201900802).

■ REFERENCES

(1) Du, J.; Gao, L.; Yang, Y.; Guo, S.; Chen, J.; Omran, M.; Chen, G. Modeling and kinetics study of microwave heat drying of low grade manganese ore. *Adv. Powder Technol.* **2020**, *31*, 2901−2911.

(2) Singh, V.; Reddy, K. V. K.; Tripathy, S. K.; Kumari, P.; Dubey, A. K.; Mohanty, R.; Satpathy, R. R.; Mukherjee, S. A sustainable reduction roasting technology to upgrade the ferruginous manganese ores. *J. Cleaner Prod.* **2021**, *284*, No. 124784.

(3) Sinha, M. K.; Purcell, W. Reducing agents in the leaching of manganese ores: A comprehensive review. *Hydrometallurgy* **2019**, *187*, 168−186.

(4) Zhang, X.-R.; Liu, Z.-H.; Fan, X.; Lian, X.; Tao, C.-Y. Optimization of reaction conditions for the electroleaching of manganese from low-grade pyrolusite. *Int. J. Min. Met. Matel* **2015**, *22*, 1121−1130.

(5) Zhang, X.; Liu, Z.; Wu, X.; Du, J.; Tao, C. Electric field enhancement in leaching of manganese from low-grade manganese dioxide ore: Kinetics and mechanism study. *J. Electroanal. Chem.* **2017**, *788*, 165−174.

(6) Luo, Z.; Shu, J.; Chen, M.; Wang, R.; Zeng, X.; Yang, Y.; Wang, R.; Chen, S.; Liu, R.; Liu, Z.; et al. Enhanced leaching of manganese from low-grade pyrolusite using ball milling and electric field. *Ecotoxicol. Environ. Saf.* **2021**, *211*, No. 111893.

(7) Chen, G.; Jiang, C.; Liu, R.; Xie, Z.; Liu, Z.; Cen, S.; Tao, C.; Guo, S. Leaching kinetics of manganese from pyrolusite using pyrite as a reductant under microwave heating. *Sep. Purif. Technol.* **2021**, *277*, No. 119472.

(8) Lan, J.; Sun, Y.; Du, Y.; Du, D.; Zhang, T. C.; Li, J. Environmentally-friendly bioleaching of manganese from pyrolusite: Performance and mechanisms. *J. Cleaner Prod.* **2020**, *249*, No. 119354.

(9) Haghighatlari, M.; Li, J.; Heidar-Zadeh, F.; Liu, Y.; Guan, X.; Head-Gordon, T. Learning to Make Chemical Predictions: the Interplay of Feature Representation, Data, and Machine Learning Methods. *Chem* **2020**, *6*, 1527−1542.

(10) Qian, X.; Yang, R. Machine learning for predicting thermal transport properties of solids. *Mater. Sci. Eng. R Rep.* **2021**, *146*, No. 100642.
(11) Packwood, D.; Nguyen, L. T. H.; Cesana, P.; Zhang, G.; Staykov, A.; Fukumoto, Y.; Nguyen, D. H. Machine Learning in Materials Chemistry: An Invitation. *Mach. Learn Appl.* **2022**, *8*, 100265.
(12) Callaghan, S. Preview of machine learning the quantum-chemical properties of metal-organic frameworks for accelerated materials discovery. *Patterns* **2021**, *2*, No. 100239.
(13) Vivanco-Benavides, L. E.; Martínez-González, C. L.; Mercado-Zúñiga, C.; Torres-Torres, C. Machine learning and materials informatics approaches in the analysis of physical properties of carbon nanotubes: A review. *Comp. Mater. Sci.* **2022**, *201*, No. 110939.
(14) Taoufik, N.; Boumya, W.; Achak, M.; Chennouk, H.; Dewil, R.; Barka, N. The state of art on the prediction of efficiency and modeling of the processes of pollutants removal based on machine learning. *Sci. Total Environ.* **2021**, *807*, 150554.
(15) Hoseinian, F. S.; Abdollahzade, A.; Mohamadi, S. S.; Hashemzadeh, M. Recovery prediction of copper oxide ore column leaching by hybrid neural genetic algorithm. *Trans. Nonferrous Met. Soc. China* **2017**, *27*, 686−693.
(16) Xie, Y.; Yu, J.; Xie, S.; Huang, T.; Gui, W. On-line prediction of ferrous ion concentration in goethite process based on self-adjusting structure RBF neural network. *Neural Netw.* **2019**, *116*, 1−10.
(17) Dai, J.; Chen, N.; Luo, B.; Gui, W.; Yang, C. Multi-scale local LSSVM based spatiotemporal modeling and optimal control for the goethite process. *Neurocomputing* **2020**, *385*, 88−99.
(18) Daware, S.; Chandel, S.; Rai, B. A machine learning framework for urban mining: A case study on recovery of copper from printed circuit boards. *Miner. Eng.* **2022**, *180*, No. 107479.
(19) Guo, Z.; Zhang, Y.; Xu, R.; Xie, H.; Xiao, X.; Peng, C. Contamination vertical distribution and key factors identification of metal(loid)s in site soil from an abandoned Pb/Zn smelter using machine learning. *Sci. Total Environ.* **2023**, *856*, No. 159264.
(20) Mokarian, P.; Bakhshayeshi, I.; Taghikhah, F.; Boroumand, Y.; Erfani, E.; Razmjou, A. The advanced design of bioleaching process for metal recovery: A machine learning approach. *Sep. Purif. Technol.* **2022**, *291*, No. 120919.
(21) Apostoluk, W.; Bartecki, A. Application of regression analysis methods for interpretation of extraction equilibria. *Hydrometallurgy* **1986**, *17*, 51−60.
(22) Flores-Sosa, M.; León-Castro, E.; Merigó, J. M.; Yager, R. R. Forecasting the exchange rate with multiple linear regression and heavy ordered weighted average operators. *Knowl-Based Syst.* **2022**, *248*, No. 108863.
(23) Jain, S.; Rathee, S.; Kumar, A.; Sambasivam, A.; Boadh, R.; Choudhary, T.; Kumar, P.; Kumar Singh, P. Prediction of temperature for various pressure levels using ANN and multiple linear regression techniques: A case study. *Mater. Today: Proc.* **2022**, *56*, 194−199.
(24) Li, H.; Liang, Y.; Xu, Q. Support vector machines and its applications in chemistry. *Chemom. Intell. Lab. Syst.* **2009**, *95*, 188−198.
(25) Cherkassky, V. The nature of statistical learning theory. *IEEE Trans. Neural Netw. Learn Syst.* **1997**, *8*, 1564−1564.
(26) Demergasso, C.; Véliz, R.; Galleguillos, P.; Marín, S.; Acosta, M.; Zepeda, V.; Zeballos, J.; Henríquez, F.; Pizarro, R.; Bekios-Calfa, J. Decision support system for bioleaching processes. *Hydrometallurgy* **2018**, *181*, 113−122.
(27) Song, Y. Y.; Lu, Y. Decision tree methods: applications for classification and prediction. *Shanghai Arch. Psychiatry* **2015**, *27*, 130−135.
(28) Coşgun, A.; Günay, M. E.; Yıldırım, R. Analysis of lipid production from Yarrowia lipolytica for renewable fuel production by machine learning. *Fuel* **2022**, *315*, No. 122817.
(29) Mingers, J. An Empirical Comparison of Selection Measures for Decision-Tree Induction. *Mach. Learn.* **1989**, *3*, 319−342.
(30) Breiman, L. Random Forests. *Mach. Learn.* **2001**, *45*, 5−32.
(31) Zhang, Z.; Wang, G.; Liu, C.; Cheng, L.; Sha, D. Bagging-based positive-unlabeled learning algorithm with Bayesian hyperparameter optimization for three-dimensional mineral potential mapping. *Comput. Geosci.* **2021**, *154*, No. 104817.
(32) Jemwa, G. T.; Aldrich, C. Monitoring of an industrial liquid−liquid extraction system with kernel-based methods. *Hydrometallurgy* **2005**, *78*, 41−51.
(33) Aydın Temel, F.; Cağcağ Yolcu, Ö.; Kuleyin, A. A multilayer perceptron-based prediction of ammonium adsorption on zeolite from landfill leachate: Batch and column studies. *J. Hazard. Mater.* **2021**, *410*, No. 124670.
(34) Hinton, G. E. Connectionist learning procedures. *Artif. Intell.* **1989**, *40*, 185.
(35) Bengio, Y.; Glorot, X.Understanding the difficulty of training deep feed forward neural networks. In *13th International Conference on Artificial Intelligence and Statistics (AISTATS)*, Sardinia; 2010.
(36) He, J.; Wang, L.; Zhang, C.; Sun, W.; Yin, Z.; Zhang, H.; Chen, D.; Pei, Y. A high throughput screening model of solidophilic flotation reagents for chalcopyrite based on quantum chemistry calculations and machine learning. *Miner. Eng.* **2022**, *177*, No. 107375.
(37) Friedman, J. H. Greedy Function Approximation: A Gradient Boosting Machine. *Ann. Stat.* **2001**, *29*, 1189−1232.
(38) Janosky, J. E. Pearson correlation coefficients vs reliability coefficients. *J. Am. Diet. Assoc* **1991**, *91*, 913.
(39) Keshavarz, S.; Faraji, F.; Rashchi, F.; Mokmeli, M. Bioleaching of manganese from a low-grade pyrolusite ore using Aspergillus niger: Process optimization and kinetic studies. *J. Environ. Manage.* **2021**, *285*, No. 112153.
(40) Das, S. C.; Sahoo, P. K.; Rao, P. K. Extraction of manganese from low-grade manganese ores by FeSO4 leaching. *Hydrometallurgy* **1982**, *8*, 35−47.
(41) Ma, W.; Tao, C.; Li, H.; Liu, Z.; Liu, R.Dynamics analysis of extraction of manganese intensified by electric field. In *2nd International Conference on Materials Science, Energy Technology, Power Engineering (MEP)*, Hangzhou; 2018.
(42) Lin, S.; Gao, L.; Yang, Y.; Chen, J.; Guo, S.; Omran, M.; Chen, G. Efficiency and sustainable leaching process of manganese from pyrolusite-pyrite mixture in sulfuric acid systems enhanced by microwave heating. *Hydrometallurgy* **2020**, *198*, No. 105519.

https://doi.org/10.1021/acsomega.2c06129
ACS Omega 2022, 7, 48130−48138